DE GRUYTER OPEN

The influence of VO_2(B) nanobelts on thermal decomposition of ammonium perchlorate

YIFU ZHANG[1*], XIANFANG TAN[2], CHANGGONG MENG[1]

[1]School of Chemistry, Dalian University of Technology, Dalian 116024, PR China
[2]Department of English, Dalian Neusoft University of Information, Dalian 116023, PR China

The influence of vanadium dioxide VO_2(B) on thermal decomposition of ammonium perchlorate (AP) has not been reported before. In this contribution, the effect of VO_2(B) nanobelts on the thermal decomposition of AP was investigated by the Thermo-Gravimetric Analysis and Differential Thermal Analysis (TG/DTA). VO_2(B) nanobelts were hydrothermally prepared using peroxovanadium (V) complexes, ethanol and water as starting materials. The thermal decomposition temperatures of AP in the presence of 1 wt.%, 3 wt.% and 6 wt.% of as-obtained VO_2(B) nanobelts were reduced by 39 °C, 62 °C and 74 °C, respectively. The results indicated that VO_2(B) nanobelts had a great influence on the thermal decomposition temperature of AP. Furthermore, the influence of the corresponding V_2O_5, which was obtained by thermal treatment of VO_2(B) nanobelts, on the thermal decomposition of AP was also investigated. The results showed that VO_2(B) nanobelts had a greater influence on the thermal decomposition temperature of AP than that of V_2O_5.

Keywords: *VO_2(B); ammonium perchlorate; thermal analysis; hydrothermal synthesis*

1. Introduction

Ammonium perchlorate (AP) is the most common oxidizing agent which has been used in various solid propellants. Thermal decomposition properties of AP influence the combustion behavior of the solid propellants. It was reported that the low-temperature thermal decomposition of AP can be accelerated by some transition metals, transition metal oxides and their related compounds (e.g. Fe_2O_3, CuO, CoO, Fe_2O_3/C, etc.) as the additives to which the thermal decomposition of AP is extremely sensitivite [1–5]. Liu et al. [6] reported that Cu, Al and Ni particles can lower the thermal decomposition temperature (T_d) of AP to 347, 425 and 364 °C, respectively. The T_d of AP was reduced to 358 °C by Cu/Fe hydrotalcite-derived mixed oxides [7]. Han et al. [8] reported that CeO_2 can reduce the T_d of AP to 390 °C. Lu et al. [9] reported that ZnO can reduce T_d of AP to 416 °C. Zhang et al. [1] obtained T_d reduction of AP to 380 °C using α-Fe_2O_3 particles. Liu et al. [10]

reported that Mg–H_2 and Mg_2NiH_4 can reduce the T_d of AP to 408 and 363 °C, respectively. Although the effect of transition metals, their oxides and related compounds on the thermal decomposition of AP has been studied to find new catalysts for AP decomposition, the issue is still meaningful for material scientists [4]. To the best of our knowledge, vanadium oxides and their derivatives used as the additives in the thermal decomposition of AP have been rarely reported [11–13]. Recently, vanadium oxides have attracted a great deal of attention. Vanadium oxide hydrate ($V_3O_7 \cdot H_2O$) nanobelts [12], V_2O_5 nanowires [13] and vanadium sesquioxide (V_2O_3) particles [11] were reported to reduce the T_d of AP to 383, 368 and 407 °C, respectively. However, to our best knowledge, the influence of VO_2(B) on the thermal decomposition of AP has not been reported yet.

VO_2(B), one of metastable phases of vanadium dioxide VO_2, has attracted increasing interest in recent years because of its layered structure and promising properties in the nanometer regime [14–23]. VO_2(B) is an attractive material for various applications, especially as an electrode

---
*E-mail: yfzhang@dlut.edu.cn

material for Li-ion battery, not only due to its proper electrode potential, but also its tunnel structure, through which Li-ions can make intercalation and de-intercalation in the reversible Li-ion battery [24, 25]. Besides, VO$_2$(B) is usually used as a precursor to be transformed to other vanadium oxides by hydrothermal or thermal treatment [26–28]. However, to the best of our knowledge, there is no report on the investigations of the influence of VO$_2$(B) on the thermal decomposition of AP. In this contribution, we have synthesized VO$_2$(B) nanobelts by a facile one-pot hydrothermal approach. Then, the as-obtained VO$_2$(B) nanobelts were explored as the additive in the thermal decomposition of AP.

2. Experimental

2.1. Synthesis

Vanadium pentoxide (V$_2$O$_5$), ethanol, hydrogen peroxide (H$_2$O$_2$, 30 wt.%) and ammonium perchlorate (AP) of an analytical grade were purchased from Sinopharm Chemical Reagent Co., Ltd., and used without any further purification. The synthesis of VO$_2$(B) nanobelts was based on the previous report [25]. In a typical synthesis, 0.455 g of bulk V$_2$O$_5$ was dispersed into 26 mL of redistilled water with magnetic stirring. Then, 2.0 mL of H$_2$O$_2$ (30 wt.%) and 2.0 mL of ethanol were successively added to the solution. The solution was still stirred for 1 h at room temperature to get good homogeneity. The mixture was then transferred to a 50 mL Teflon lined stainless steel autoclave, then sealed and maintained at 180 °C for 48 h. When the reaction was finished, the blue-black precipitates were filtered off, washed with distilled water and anhydrous alcohol several times, and dried in vacuum at 75 °C.

2.2. Characterization

X-ray powder diffraction (XRD) was carried out on a D8 X-ray diffractometer equipment with CuKα radiation, λ = 1.54060 Å. The data were collected between 10° and 70° with a scan speed of 4°/min. X-ray photoelectron spectroscopy (XPS) was performed using KRATOS, XSAM800

with an exciting source of MgKα (1253.6 eV, 16 mA·12 kV). The morphology of the products was studied by scanning electron microscopy (SEM, Quanta 200) and transmission electron microscopy (TEM, JEM-2100). The sample was dispersed in absolute ethanol and was ultrasonicated before TEM. Thermo-Gravimetric Analysis and Differential Thermal Analysis (TG/DTA) were performed on SETSYS-1750 (AETARAM Instruments). About 5 mg of VO$_2$(B) and AP mixture were heated in an Al$_2$O$_3$ crucible in nitrogen atmosphere from ambient temperature to 500 °C at a constant rise of temperature (10 °C/min). AP and VO$_2$(B) were mixed at a mass ratio of 99:1, 97:3 and 94:6, and ground to make them dispersed homogeneously in order to prepare the target samples for thermal decomposition analyses.

3. Results and discussion

Fig. 1 shows a typical XRD pattern of an as-obtained sample, and all the diffraction peaks can be readily indexed to the monoclinic crystalline phase (space group C2/m) of VO$_2$(B) (JCPDS Card No. 65-7960) [29]. No peaks of any other phases, such as V$_2$O$_5$, V$_3$O$_7$, VO$_2$(A), VO$_2$(M) and V$_2$O$_3$, have been detected, revealing high purity of the as-prepared VO$_2$(B) sample.
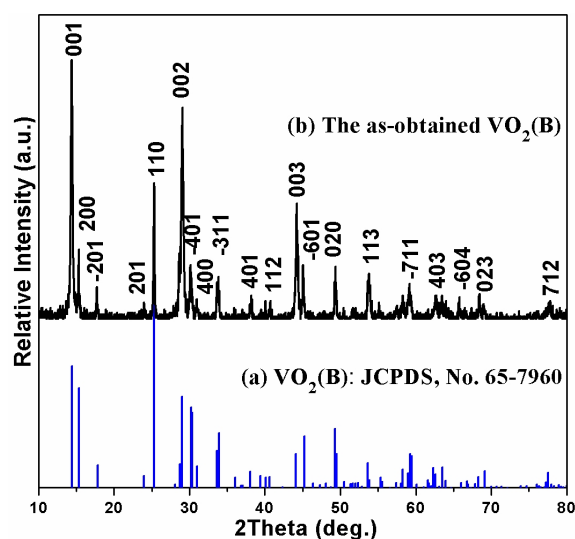

Fig. 1. XRD patterns of the as-obtained VO$_2$(B).

Further data about the composition and vanadium valence state of the surface of the as-obtained $VO_2(B)$ were collected by XPS (Fig. 2), which reveals that the sample consists only of vanadium and oxygen (C_{1s} peak is due to some carbon dioxides absorbed on the surface and can be disregarded). The peaks centered at 516.2 eV, 523.2 eV and 529.1 eV are attributed to the $V_{2p3/2}$, $V_{2p1/2}$ and O_{1s}, respectively. The binding energy at 516.2 eV and 523.2 eV are characteristic of vanadium in the +4 oxidation state [30]. Besides, it has been established that the oxidation state of vanadium oxides could be determined by the distance of binding energy level (Δ) between the O_{1s} and $V_{2p3/2}$ [31]. As for this sample, the $\Delta(O_{1s}-V_{2p3/2})$ value is 12.9 eV, which well corresponds to the reported value of V^{4+} in the literature [31]. The result further confirms the vanadium valence to be at the +4 oxidation state, in agreement with XRD results.
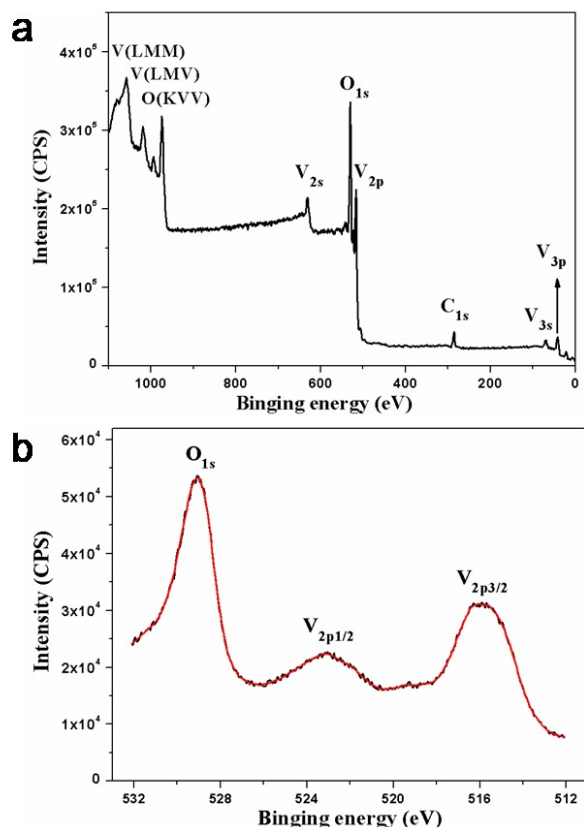
Fig. 3 shows typical SEM and TEM images of the as-prepared $VO_2(B)$. The SEM image (Fig. 3a) indicates that the as-obtained $VO_2(B)$ consists of a large number of nanosheets which are made up of nanobelts, and rectangular cross sections can be occasionally observed. The TEM images (Fig. 3b – 3d) reveal that $VO_2(B)$ contains lots of 1D nanobelts, which is consistent with the observation of SEM. SEM and TEM results confirm that $VO_2(B)$ nanobelts grow well separated, show high crystallinity degree, and have the length in the range of several to tens of micrometers, width of 80 to 220 nm and thickness of 10 to 25 nm. Furthermore, the microstructure of $VO_2(B)$ nanobelts was studied by the high-resolution TEM, as shown in Fig. 3e. The interplanar distance d = 0.352 nm is in agreement with the d_{110} spacing of $VO_2(B)$. Therefore, the as-obtained $VO_2(B)$ nanobelts grow along the [010] direction in agreement with previous reports [14, 32].
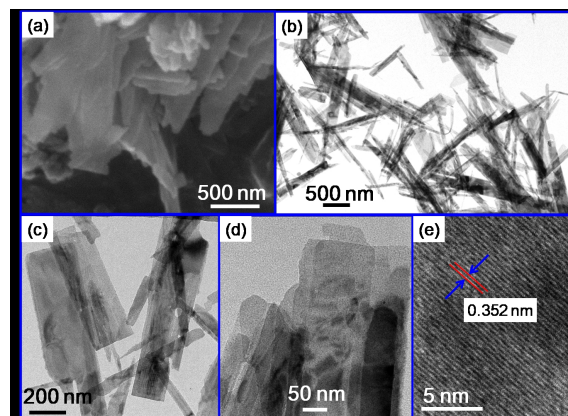

Fig. 3. The morphology of the as-obtained $VO_2(B)$: (a) SEM image; (b – d) TEM images; (e) HRTEM image.

Furthermore, the as-synthesized $VO_2(B)$ nanobelts were explored as an additive in the thermal decomposition of AP. TG and DTG curves of pure AP and AP in the presence of $VO_2(B)$ (1 wt.%, 3 wt.% and 6 wt.%) are shown in Fig. 4. The starting decomposition temperature of AP is obviously reduced by the addition of $VO_2(B)$, however, the amount of $VO_2(B)$ has little influence on the starting decomposition temperature of AP. However, it can be clearly observed from Fig. 4a

Fig. 2. XPS spectra of the as-obtained $VO_2(B)$: (a) survey spectrum; (b) core-level spectrum.

that the addition of VO$_2$(B) to AP leads to a significant reduction of the ending decomposition temperature of AP (pure AP: 464 °C; 1% VO$_2$(B) + 99% AP: 420 °C; 3% VO$_2$(B) + 97% AP: 401 °C; and 6% VO$_2$(B) + 94% AP: 387 °C). Fig. 4b shows the corresponding DTG curves and two peaks can be seen in each curve, which reveals that the thermal decomposition of AP contains two steps. Further information on the influence of VO$_2$(B) nanobelts on decomposition of AP was provided by heat flow curves, as shown in Fig. 5. The exothermic peaks at 318 °C and 456 °C in pure AP (Fig. 5a) are assigned to the partial decomposition of AP leading to some intermediate products, such as NH$_3$ and HClO$_4$, and then complete decomposition to volatile products [33], which is in agreement with the TG and DTG curves in Fig. 4. However, the obvious changes with the addition of different amounts of VO$_2$(B) to AP can be observed (Fig. 5). With addition of 1 wt.%, 3 wt.% and 6 wt.% of VO$_2$(B), the thermal decomposition temperature of AP is lowered to 417 °C, 394 and 382 °C (decreased by 39 °C, 62 °C and 74 °C), respectively. Thus, we can conclude that VO$_2$(B) has a great influence on the thermal decomposition of AP, and it may be used as a promising additive in the future. Comparing Fig. 5 with Fig. 4, it can be seen that there is no weight loss at the endothermic peak located at 247 °C, which is due to the transition from orthorhombic to cubic AP [4] and is not influenced by the additives.

According to the previous studies [1, 4, 5, 34], the decomposition of AP consists of essentially three steps:

1. 240 to 250 °C: crystal transformation from orthorhombic to cubic phase;
2. 300 to 330 °C: the first decomposition step: a solid-gas multiphase reaction including decomposition and sublimation: NH$_4$ClO$_4$ $\rightarrow$ NH$_4^+$ + ClO$_4^-$ $\rightarrow$ NH$_3$(g) + HClO$_4$(g);
3. 450 to 480 °C: the second decomposition step: NH$_3$ and HClO$_4$ react after entering the gas phase, and the products are N$_2$O, O$_2$, Cl$_2$, H$_2$O and small amount of NO.
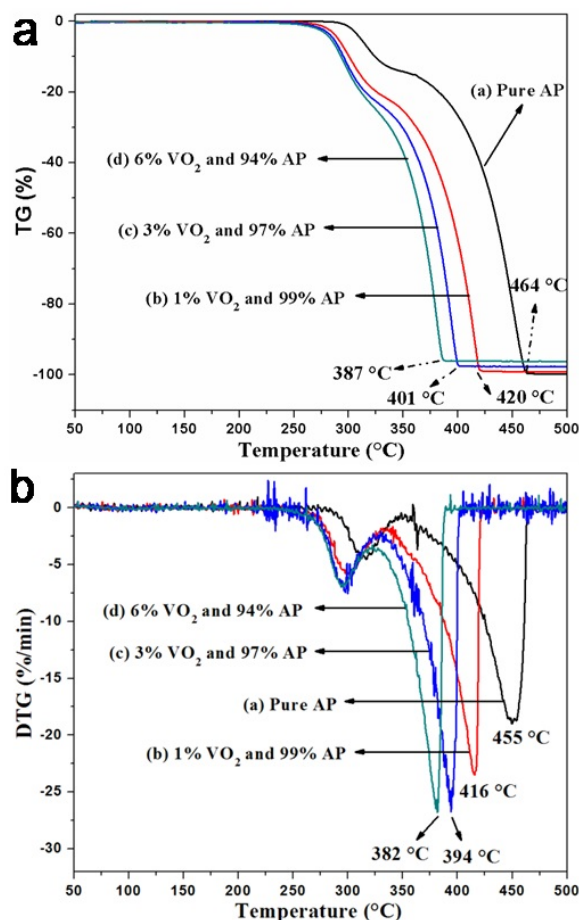

Fig. 4. TG and DTG curves showing the influence of VO$_2$(B) nanobelts on decomposition of AP.

From our experimental results we can deduce that the additives can accelerate the thermal decomposition of AP via the third step, because the temperature of the high temperature exothermic decomposition process is greatly reduced. Up to now, the thermal decomposition mechanism of AP has not been fully understood because the decomposition is a complex hetero-phase process involving coupled reactions in the solid, adsorbed and gaseous phases. There still remain some unsolved issues. According to the traditional electron-transfer theory [4], the presence of partially filled 3d orbital in vanadium atom provides help in the electron transfer process. Positive hole in vanadium atom can accept electrons from AP ion and its intermediate products by which the thermal decomposition of AP is accelerated. However, in case of
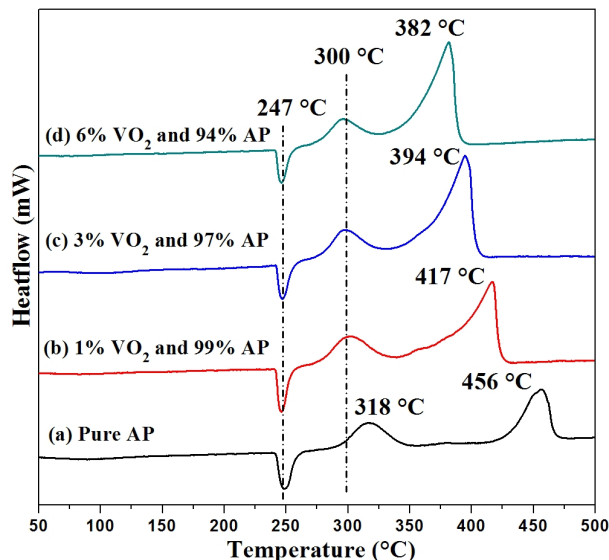
Fig. 5. Heat flow curves showing the influence of VO$_2$(B) nanobelts on decomposition of AP.

VO$_2$(B) nanobelts, there may be another reason except the mentioned one. The reason is that VO$_2$(B) reacts with AP, which can also accelerate the thermal decomposition of AP. The above inference is proved by Fig. 6. The product obtained after decomposition of AP with VO$_2$(B) nanobelts was the yellow residue V$_2$O$_5$. Fig. 6 discloses the influence of VO$_2$(B) and the corresponding V$_2$O$_5$ on decomposition of AP, and it reveals that reduction of the thermal decomposition temperature of AP by VO$_2$(B) is lower than that of V$_2$O$_5$. The above results indicate that VO$_2$(B) can react with AP, which accelerates the thermal decomposition of AP. The VO$_2$(B) has a great influence on the thermal decomposition of AP, and the mechanism is probably caused by two reasons: (1) the presence of partially filled 3d orbital in vanadium atom which helps in the electron transfer process, based on the traditional electron-transfer theory; (2) VO$_2$(B) nanobelts reaction with AP to release heat. These two reasons can accelerate the thermal decomposition of AP.

4. Conclusions

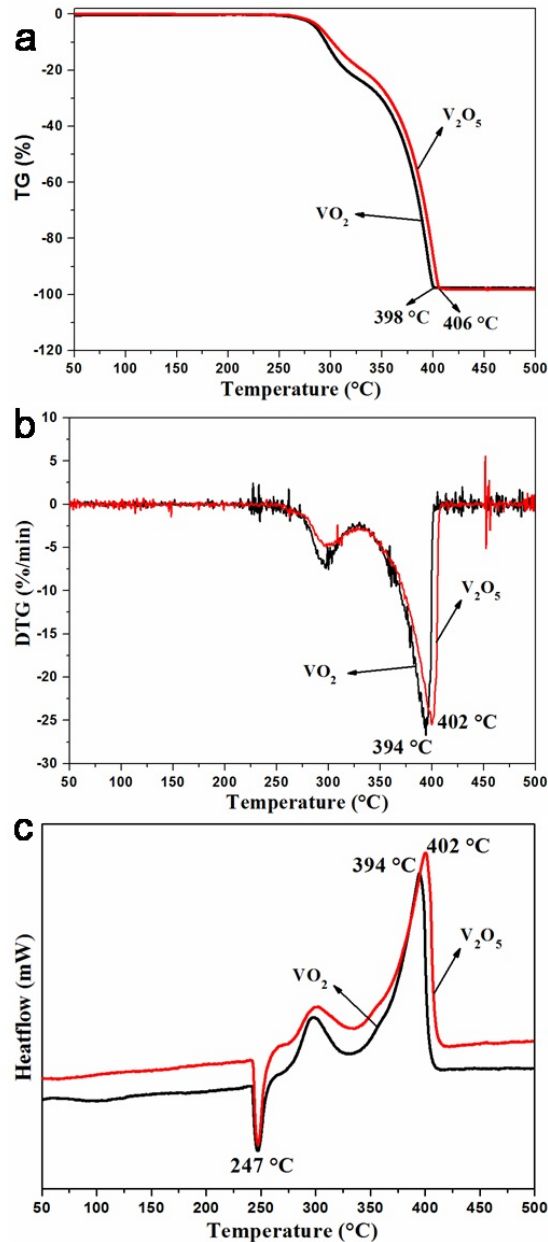In conclusion, the effect of VO$_2$(B) nanobelts on thermal decomposition of AP was investigated

Fig. 6. TG, DTG and heat flow curves showing the influence of the as-obtained VO$_2$(B) nanobelts and V$_2$O$_5$ on decomposition of AP; the mass ratio of the additive is 3 %. Note that V$_2$O$_5$ was obtained by thermal treatment of VO$_2$(B) nanobelts.

by the TG/DTA analysis. The thermal decomposition temperatures of AP in the presence of 1 wt.%, 3 wt.% and 6 wt.% of VO$_2$(B) nanobelts were reduced to 417, 394 and 382 °C (decreased by 39 °C, 62 °C and 74 °C), respectively. We can conclude

that VO$_2$(B) had a great influence on the thermal decomposition of AP, and it may be used as a promising additive in the future. Finally, the thermal decomposition mechanism of AP based on the traditional electron-transfer theory and VO$_2$(B) reacting with AP was proposed.

Acknowledgements

References

[1] ZHANG Y., LIU X., NIE J., YU L., ZHONG Y., HUANG C., *J. Solid State Chem.*, 184 (2011), 387.

[2] LI L.P., SUN X.F., QIU X.Q., XU J.X., LI G.S., *Inorg. Chem.*, 47 (2008), 8839.

[3] ZHOU Z., TIAN S., ZENG D., TANG G., XIE C., *J. Alloy. Compd.*, 513 (2012), 213.

[4] BOLDYREV V.V., *Thermochim. Acta*, 443 (2006), 1.

[5] CHEN L.J., LI L.P., LI G.S., *J. Alloy. Compd.*, 464 (2008), 532.

[6] LIU L.L., LI F.S., TAN L.H., MING L., YI Y., *Propell. Explos. Pyrot.*, 29 (2004), 34.

[7] LIU H., JIAO Q., ZHAO Y., LI H., SUN C., LI X., WU H., *Mater. Lett.*, 64 (2010), 1698.

[8] HAN Z.-W., HAN Y.-C., XU S., *J. Therm. Anal. Calorim.*, 113 (2) (2013), 673.

[9] LU J., ZHU J., WANG Z., CAO J., ZHOU X., *Ceram. Int.*, 40 (1B) (2014), 1489.

[10] LIU L., XIN J., MA F., ZHI C., LI F., *Propell. Explos. Pyrot.*, 38 (5) (2013), 629.

[11] ZHANG Y., ZHANG J., NIE J., ZHONG Y., LIU X., HUANG C., *Micro Nano Lett.*, 7 (2012), 782.

[12] ZHANG Y., LIU X., CHEN D., YU L., NIE J., YI S., LI H., HUANG C., *J. Alloy. Compd.*, 509 (2011), L69.

[13] ZHANG Y., WANG N., HUANG Y., WU W., HUANG C., MENG C., *Ceram. Int.*, 40 (2014) 11393.

[14] LIU J.F., LI Q.H., WANG T.H., YU D.P., LI Y.D., *Angew. Chem. Int. Edit.*, 43 (2004), 5048.

[15] ZHANG Y., FAN M., ZHOU M., HUANG C., CHEN C., CAO Y., XIE G., LI H., LIU X., *Bull. Mater. Sci.*, 35 (2012), 369.

[16] MYUNG S., LEE M., KIM G.T., HA J.S., HONG S., *Adv. Mater.*, 17 (2005), 2361.

[17] ZHANG Y., FAN M., LIU X., HUANG C., LI H., *Eur. J. Inorg. Chem.*, 2012 (2012), 1650.

[18] ZHANG Y., ZHANG J., ZHANG X., MO S., WU W., NIU F., ZHONG Y., LIU X., HUANG C., LIU X., *J. Alloy. Compd.*, 570 (2013), 104.

[19] STRELCOV E., LILACH Y., KOLMAKOV A., *Nano Lett.*, 9 (2009), 2322.

[20] ZHANG Y., HUANG Y., ZHANG J., WU W., NIU F., ZHONG Y., LIU X., LIU X., HUANG C., *Mater. Res. Bull.*, 47 (2012), 1978.

[21] ZHANG Y., CHEN C., ZHANG J., HU L., WU W., ZHONG Y., CAO Y., LIU X., HUANG C., *Curr. Appl. Phys.*, 13 (2013), 47.

[22] ZHANG Y., ZHANG J., ZHANG X., HUANG C., ZHONG Y., DENG Y., *Mater. Lett.*, 92 (2013), 61.

[23] LIU X., XIE G., HUANG C., XU Q., ZHANG Y., LUO Y., *Mater. Lett.*, 62 (2008), 1878.

[24] NI J.A., JIANG W.T., YU K., GAO Y.F., ZHU Z.Q., *Electrochim. Acta*, 56 (2011), 2122.

[25] ZHANG Y., CHEN C., WU W., NIU F., LIU X., ZHONG Y., CAO Y., LIU X., HUANG C., *Ceram. Int.*, 39 (2013), 129.

[26] ZHANG Y., LI W., FAN M., ZHANG F., ZHANG J., LIU X., ZHANG H., HUANG C., LI H., *J. Alloy. Compd.*, 544 (2012), 30.

[27] ZHANG Y., FAN M., LIU X., XIE G., LI H., HUANG C., *Solid State Commun.*, 152 (2012), 253.

[28] ZHANG Y., ZHANG X., HUANG Y., HUANG C., NIU F., MENG C., TAN X., *Solid State Commun.*, 180 (2014), 24.

[29] THEOBALD F., CABALA R., BERNARD J., *J. Solid State Chem.*, 17 (1976), 431.

[30] WAGNER C.D., RIGGS W.M., DAVIS L.E., MOULDER J.F., *Handbook of X-ray Photoelectrom Spectroscopy*, Perkin-Elmer Corporation, Minnesota, 1979.

[31] MENDIALDUA J., CASANOVA R., BARBAUX Y., *J. Electron. Spectrosc.*, 71 (1995), 249.

[32] LEROUX C., NIHOUL G., TENDELOO VAN G., *Phys. Rev. B*, 57 (1998), 5111.

[33] SHI X.Q., JIANG X.H., LU L.D., YANG X.J., WANG X., *Mater. Lett.*, 62 (2008), 1238.

[34] SONG L.M., ZHANG S.J., CHEN B., GE J.J., JIA X.C., *Colloid. Surface. A*, 360 (2010), 1.